Combined Classical and Quantum Accelerometers for Future Satellite Gravity Missions

Alireza Hosseiniarani, Manuel Schilling, Benjamin Tennstedt, Alexey Kupriyanov, Quentin Beaufils, Annike Knabe, Arpetha C. Sreekantaiah, Franck Pereira dos Santos, Steffen Schön, Jürgen Müller

Earth and Space Science

RESEARCH ARTICLE
10.1029/2024EA004187

Combined Classical and Quantum Accelerometers for Future Satellite Gravity Missions

Alireza HosseiniArani[1], Manuel Schilling[2], Benjamin Tennstedt[1], Alexey Kupriyanov[1], Quentin Beaufils[3], Annike Knabe[1], Arpetha C. Sreekantaiah[1], Franck Pereira dos Santos[3], Steffen Schön[1], and Jürgen Müller[1]

[1]Leibniz University Hannover, Institut für Erdmessung (IfE), Hannover, Germany, [2]German Aerospace Center (DLR), Institute for Satellite Geodesy and Inertial Sensing, Hannover, Germany, [3]LNE-SYRTE, Observatoire de Paris, Université PSL, CNRS, Sorbonne Université, Paris, France

Key Points:

- An extended Kalman-filter based concept for hybridization of classical and quantum accelerometer is presented
- The simulation of the quantum sensor is based on a detailed error model that accounts for various noise sources and rotational effects
- The benefit of the improved sensor to gravity field recovery is discussed and necessary prerequisites are evaluated

Correspondence to:
A. HosseiniArani,
hosseiniarani@ife.uni-hannover.de

Citation:
HosseiniArani, A., Schilling, M., Tennstedt, B., Kupriyanov, A., Beaufils, Q., Knabe, A., et al. (2025). Combined classical and quantum accelerometers for future satellite gravity missions. *Earth and Space Science*, *12*, e2024EA004187. https://doi.org/10.1029/2024EA004187

Received 10 JAN 2025
Accepted 9 APR 2025

Author Contributions:
Conceptualization: Manuel Schilling, Steffen Schön, Jürgen Müller
Formal analysis: Alireza HosseiniArani
Funding acquisition: Jürgen Müller
Investigation: Alireza HosseiniArani, Manuel Schilling, Alexey Kupriyanov, Annike Knabe
Methodology: Alireza HosseiniArani, Manuel Schilling, Benjamin Tennstedt, Quentin Beaufils, Franck Pereira dos Santos, Steffen Schön
Project administration: Jürgen Müller
Software: Alireza HosseiniArani, Manuel Schilling, Benjamin Tennstedt, Arpetha C. Sreekantaiah
Supervision: Manuel Schilling, Franck Pereira dos Santos, Steffen Schön, Jürgen Müller
Validation: Alireza HosseiniArani, Quentin Beaufils, Franck Pereira dos Santos, Steffen Schön, Jürgen Müller
Visualization: Alireza HosseiniArani, Alexey Kupriyanov

Abstract Cold atom interferometry based quantum accelerometers (Q-ACCs) are very promising for future satellite gravity missions thanks to their strength in providing long-term stable and precise measurements of non-gravitational accelerations. However, their limitations due to the low measurement rate and the existence of ambiguities in the raw sensor measurements call for hybridization of the Q-ACC with a classical one (e.g., electrostatic) with higher bandwidth. While previous hybridization studies have so far considered simple noise models for the Q-ACC and neglected the impact of satellite rotation on the phase shift of the accelerometer, we perform here a more advanced hybridization simulation by implementing a comprehensive noise model for the satellite-based Q-ACCs and considering the full impact of rotation, gravity gradient, and self-gravity on the instrument. We perform simulation studies for scenarios with different assumptions about quantum and classical sensors and satellite missions. The performance benefits of the hybrid solutions, taking the synergy of both classical and Q-ACCs into account, will be quantified. We found that implementing a hybrid accelerometer onboard a future gravity mission improves the gravity solution by one to two orders in lower and higher degrees. In particular, the produced global gravity field maps show a drastic reduction in the instrumental contribution to the striping effect after introducing measurements from the hybrid accelerometers.

1. Introduction

1.1. Next Generation of Satellite Gravity Missions

Satellite gravimetry missions play a crucial role in monitoring the Earth's gravity field and its temporal changes. Missions such as GRACE (-FO) have significantly contributed to the understanding of mass variations associated with climate change (Humphrey et al., 2023; Scanlon et al., 2023; Tapley et al., 2019) and gave insights into the Earth's interior processes (Lecomte et al., 2023; Mandea et al., 2020). The current solutions of the gravity field offered by these missions are limited, particularly at very low degrees such as C_{20} and even extending to C_{30} in times when only one operational accelerometer is available on two satellites (Loomis et al., 2020).

The C_{20} coefficient is an expression of the oblateness of the Earth and the accelerometer performance is already limited at orbital frequency (see also Figure 1). C_{30} describes the pear-shaped form of the Earth. It reflects hemispherical mass asymmetries, which may be influenced by continental water storage changes and large-scale climate shifts. While the C_{30} degradation appears to be mostly related to the availability of accelerometers on both satellites, the reason for the poor determination of C_{20} in GRACE (-FO) is at least partly unknown (Loomis et al., 2019). In addition, temporal variations of C_{20}, for example, due to secular mass trends, are not well represented in GRACE (-FO) solutions compared to satellite laser-ranging solutions (SLR) of C_{20}. The GRACE C_{20} time series also contains a periodic signal with an approximately 161 day period. SLR on the other hand already provides the time variability of C_{20} for several decades longer than GRACE without such a signal. For the behavior of the GRACE C_{20} solution several explanations were already investigated, for example, an aliasing effect originating in the ocean tides or accelerometer errors (a brief overview is given in Loomis et al., 2019). Consequently, these coefficients are often substituted with values from gravity field solutions. Another challenge appears due to the drift in low frequencies of the electrostatic accelerometers employed in the GRACE (-FO) missions, thereby constraining the gravity field solution. In general, the spatial resolution remains confined to areas of a few hundreds of kilometer (Chen et al., 2022) for a signal amplitude of 10 mm equivalent water height (EWH) in typical monthly gravity field solutions. To meet the demands of the scientific community, future

Writing – original draft:
Alireza HosseiniArani, Manuel Schilling
Writing – review & editing:
Manuel Schilling, Benjamin Tennstedt, Alexey Kupriyanov, Quentin Beaufils, Annike Knabe, Franck Pereira dos Santos, Steffen Schön, Jürgen Müller

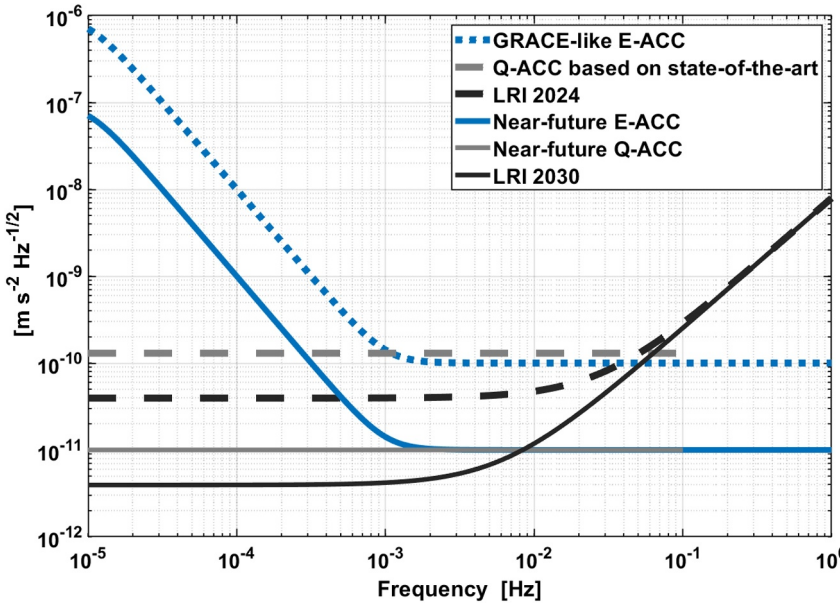

Figure 1. Amplitude spectral densities in range accelerations in the along-track direction for a GRACE-like satellite gravity mission using an electrostatic (classical) and cold atom interferometry (quantum) accelerometers for the state-of-the-art and near-future scenarios (Christophe et al., 2015; Flury et al., 2008; HosseiniArani et al., 2024); together with laser ranging systems (Abich et al., 2019; Kupriyanov, Reis, Schilling, et al., 2024).

satellite gravity missions must aim for a resolution of $(200\ \text{km})^2$ for an amplitude of 10 mm EWH or even smaller (Pail et al., 2015; Wiese et al., 2022). In this study, the primary focus is on the instrumental contributions to the gravity field mission performance. More information about the other main contributors can be found in (Haagmans et al., 2020; Shihora et al., 2022).

1.2. Quantum Accelerometer

Raman atom interferometry accelerometers implement three laser pulses acting either as beam splitters or mirror pulses (Geiger et al., 2020; Kasevich & Chu, 1991). These laser pulses consist of two counter-propagating laser beams whose frequency difference is tuned in resonance with a two-photon Raman transition between the two hyperfine ground states of an alkali atom, ^{87}Rb in our case. The first pulse of light creates a beam splitter, which places the atom in a quantum superposition of two wave packets of different momenta. A second light pulse inverts the momenta of the two wave packets after a time interval T. Finally, a second beam splitting pulse closes the interferometer after a further time interval T. The atom interferometer phase shift $\Delta\Phi$ is the result of the projection of the acceleration $\vec{a}$ experienced by the atoms along the effective optical wave vector of the laser light $\vec{k}_{\text{eff}} = \vec{k}_1 - \vec{k}_2$ which is the difference between the optical wave vectors $\vec{k}_i$ of both laser beams. The leading order of the atom interferometer phase $\Delta\Phi$ is described by

$$\Delta\Phi = (2\ k_{\text{eff}}\ a)\ T^2 + \Phi_{L,i} \tag{1}$$

with the acceleration a and $k_{\text{eff}} = |\vec{k}_{\text{eff}}|$ now expressed in direction of the counter-propagating laser beams. k_{eff} is also related to the photon momentum exchange by $\hbar k_{\text{eff}}$ where $\hbar$ is the reduced Planck constant. A factor 2 is added because we consider a double diffraction (Lévèque et al., 2009) quantum accelerometer (Q-ACC), as it is anticipated for microgravity (for more details see HosseiniArani et al., 2024). An arbitrary Raman laser phase Φ_L can be added to the last light pulse to operate the interferometer, for example, at mid-fringe as described in HosseiniArani et al. (2022).

Alternative interferometer architectures are also possible, such as those based on Bragg diffraction. Unlike Raman processes, Bragg diffraction transfers momentum between atomic wave packets without changing their internal states, thereby reducing sensitivity to magnetic field fluctuations and enabling large momentum transfer (Altin

et al., 2013). Bragg processes typically require longer pulse durations and higher laser power, which may impose technical constraints. In contrast, double diffraction Raman interferometry provides efficient symmetric beam splitting and internal state labeling, which are advantageous for suppressing systematic errors in microgravity environments (Geiger et al., 2011), but it relies on ultracold atomic ensembles to achieve high diffraction efficiency and to mitigate unwanted transitions (Hartmann et al., 2020). Both techniques are viable for space-based atom interferometry; however, in this work, we focus exclusively on Raman interferometry. Detailed comparison to the other approaches lies beyond the scope of this paper.

According to Equation 1, the sensitivity of the Q-ACC can be increased by increasing the interrogation time T. In terrestrial applications, T is limited by the length of the free fall distance of the atoms, for example, up to 300 ms for a transportable (Freier et al., 2016) and up to a couple of seconds for stationary instruments (Asenbaum et al., 2020; Schilling et al., 2020). As atoms and satellites in space are in free fall, longer separation times T are possible. There, a Q-ACC would allow for monitoring the deviation from the free fall trajectory resulting from non-gravitational accelerations acting on the satellite.

Increasing the interrogation time over seconds demands extremely low atomic temperatures on the order of tens of picokelvin (pK) or below, in order to reduce the expansion of the atomic source. Advanced cooling methods are to be employed, such as delta-kick collimation, which allowed reaching the lowest demonstarted temperatures, of around 40 pK (Deppner et al., 2021; Xie et al., 2022). Delta-kick cooling works by applying a brief harmonic potential after an initial free expansion of the atomic cloud, effectively reversing part of the velocity spread. This process collimates the cloud and significantly reduces its effective temperature without substantial atom loss (Müntinga et al., 2013). This technique is particularly advantageous in microgravity environments, where ultra-low expansion rates are essential for long interrogation times in atom interferometry and it does not significantly increase the payload weight and size.

The sensitivity limits of an atom interferometer in absolute inertial sensing have been discussed in detail by, for example, Geiger et al. (2020) and HosseiniArani et al. (2024). To be brief, with the currently available technology, a cold atom interferometry (CAI) based quantum sensor in space with some minor improvements (e.g., on the positioning of the atomic cloud) is expected to achieve sensitivity in the order of 1×10^{10} m/s^2/$\sqrt{\text{Hz}}$ in the frequency range of 1×10^{-5}Hz to 1×10^{-1}Hz. However, ongoing and future advances in atom interferometry in the next 5–10 years are expected to reach a sensitivity in the order of 1×10^{-11} m/s^2/$\sqrt{\text{Hz}}$ in the same frequency range (HosseiniArani et al., 2024; Knabe et al., 2022; Zahzam, Christophe, Lebat, et al., 2022). In Section 3, we study the hybridization of quantum sensors with conventional ones based on different assumptions for the sensitivity of the sensors.

1.3. Hybridization of the Classical and Quantum Sensors

The benefit of hybridization of cold atom and electrostatic accelerometers for gravity field missions in a simplified scenario without rotational effects has already been shown (e.g. Zingerle et al., 2024). These studies typically generate noise-only time series for the two accelerometers and combine them, for example, by filtering. The hybrid accelerometer noise, converted to ranging accelerations, is added to the ranging observations before gravity field recovery. Our method combines the (noisy) measurements of the two accelerometers while simultaneously using the measurements of the electrostatic accelerometer (E-ACC) to solve the phase ambiguities of the cold atom interferometer. The method introduced here can potentially be used in real-time scenarios for data generated by future hybrid sensors and has already been demonstrated for application in inertial navigation using a navigation-grade Inertial Measurement Unit (IMU) to emulate a CAI (Weddig et al., 2021).

In our previous study (HosseiniArani et al., 2022), we have shown the benefit of such hybridization in a simplified case for a GRACE-like mission. Here, we realize a more advanced version of the hybridization in which we use a comprehensive noise model for the Q-ACCs and model the full impact of rotation on the Q-ACC and the Kalman filter.

Three scenarios were studied: first, the hybridization of a Q-ACC based on state-of-the-art technology with a few minor improvements with an E-ACC similar to the one on-board of the GRACE-FO satellites. In the second scenario, we study the hybridization of a highly improved Q-ACC (what we expect to achieve in the next 5–10 years) with another proposed highly accurate E-ACC model. For the first two scenarios, we assumed the satellites to be at an altitude of around 480 km. In the third scenario, we assume the same sensors as the first

scenario, but the satellites were assumed to be in an orbit of 300 km altitude. The latter would show the efficiency of the filter in the presence of high-amplitude non-gravitational signals.

In Section 2, we describe our modeling for the satellite gravity missions and the classical and Q-ACCs on-board. We then discuss the modeling of the rotation, gravity gradient, and self-gravity effects. Afterward, we introduce the Kalman filter approach we use to hybridize the accelerometers' measurements and discuss the simulation of the recovery of the gravity field. In Section 3, we discuss the results of the hybridization in three different scenarios, and we compare the achievable accuracy in the gravity field recovery by introducing the hybrid accelerometer concepts on-board future satellite gravity missions.

2. Modeling

2.1. Modeling a GRACE-Like Gravity Mission

In this study, we consider a GRACE-like satellite pair in a circular polar orbit around the Earth with an altitude of 480 km. The simulation is implemented in the MATLAB/Simulink-based eXtended High-Performance satellite dynamics Simulator (XHPS, Wöske et al., 2019) developed by ZARM/DLR. XHPS calculates the orbits of a GRACE-FO mission scenario under consideration of the Earth's gravity field "EGM2008", non-gravitational accelerations (atmospheric drag, solar radiation pressure, Earth albedo and thermal radiation pressure) and the GRACE satellite geometry. To consider the effect of non-gravitational accelerations on the spacecraft, we use a detailed surface model of the satellite body included in XHPS.

2.2. Classical and Quantum Sensor Models

An E-ACC is a classical sensor that measures accelerations. If the E-ACC is placed at the satellite's center of mass, it only measures the non-gravitational accelerations acting on the satellite in three orthogonal directions (along-track, cross-track, and radial). This is because the satellite is free-falling in the Earth's gravity field. A classical or conventional E-ACC usually performs best in a frequency range higher than 1×10^{-3} Hz, while at lower frequencies, the measurements suffer from large noise. The low-frequency noise (see Figure 1) causes a bias in the measured accelerations. The accelerometer measurements, therefore, can be written as:

$$A_{ACC} = B + S \cdot A_{non\text{-}grav.} + N \tag{2}$$

where B is the accelerometer bias, S is the accelerometer scaling factor and N stands for the random noise. The scaling factor of an accelerometer refers to how its output changes in response to a known input acceleration. This scaling factor can be measured accurately in controlled calibration setups before launch and adjusted periodically during the mission by using known reference signals or maneuvers. Scaling factor calibration is usually stable over time and can be adjusted with high precision because it relies on known physical principles and predictable response to input changes. The bias of an accelerometer, on the other hand, is the output it reads when there is theoretically zero acceleration. Bias tends to be more variable and susceptible to environmental factors. Unlike scaling factors, biases are more difficult to calibrate in-flight and can drift unpredictably, making precise determination and long-term stability challenging (Christophe et al., 2009; Flury & Rummel, 2005). For this reason, in this study, we ignore the scaling factor and focus on the determination of the E-ACC bias. The sensor model of an E-ACC, based on the GRACE ACC sensitive axis (Christophe et al., 2015) with a noise level of 1×10^{-10} m/s^2/$\sqrt{\text{Hz}}$ in frequencies above 1×10^{-3} Hz, is implemented in XHPS. The sampling rate of the E-ACC is 10 Hz.

Although better performing E-ACC have already been in space (e.g. GOCE mission; Marque et al., 2010) or are published as recent developments (Christophe et al., 2018; Zahzam, Christophe, Lebat, et al., 2022), the GRACE-FO type accelerometer was chosen to later compare with GRACE-FO gravity field solutions. This is also a worst-case scenario, that is, if this method works successfully with this accelerometer, an accelerometer with lower noise at low frequencies is not a priority when enabling a hybrid accelerometer. It is worth mentioning that this type of accelerometer is now again foreseen for NASA's GRACE-C mission. Later during this study, we will also use a more accurate model of E-ACC with a noise level of 1×10^{-11} m/s^2/$\sqrt{\text{Hz}}$ above 1×10^{-3} Hz and test the performance of its hybridization with the Q-ACC model.

Table 1
Parameters of the Quantum Accelerometers Considered in Different Scenarios

Parameter	Quantum sensor based on state-of-the-art technology[a]	Near-future quantum sensor[b]
Laser Waist	10 mm	20 mm
Atomic Temperature	40×10^{-12} K	10×10^{-12} K
Number of Atoms	5×10^5	10^6
Required Laser Power	90 mW (for the π pulse)	360 mW (for the π pulse)
Error on the Positioning of the Atomic Cloud[c]	3×10^{-5} m	3×10^{-5} m
Transversal Velocity of Atoms	33×10^{-6} m s^{-1}	20×10^{-6} m s^{-1}
Error on the Measurement of Rotation Rates	2.2×10^{-7} rad s^{-1}	6.6×10^{-8} rad s^{-1}
Rotation Compensation	counter-rotating raman mirror	counter-rotation of the quantum sensor
Atomic Flight Time ($2T$)	5 s	10 s
Pointing error requirement	1×10^{-5} rad	3×10^{-6} rad

[a]In this scenario, minor improvements have been considered for the quantum sensor based on state-of-the-art technology presented in (HosseiniArani et al., 2022) to make the quantum sensor compatible with the state-of-the-art classical accelerometers. [b]We assume the near future quantum sensor as what can be achieved in the next 5–10 years (HosseiniArani et al., 2024). [c]for more information about this error please refer to (HosseiniArani et al., 2024).

In a satellite setting, the Q-ACC can be used to measure the non-gravitational accelerations acting on the satellite. A three-axis instrument could also be implemented for geodesy applications, but in this paper, we focus on a single-axis Q-ACC oriented in the along-track (X-) direction. Equation 1 describes a single-axis accelerometer phase shift in the absence of rotation of the satellite. Because of the change of the non-gravitational acceleration during the Q-ACC interrogation time, we integrate this equation by considering the sensitivity function of Q-ACC as described in Cheinet et al. (2008). To simulate the error budget of the Q-ACC, we implement a detailed noise model including the major noise sources that affect the measurement: laser frequency, wavefront aberrations, and detection noises. The details of this error-source model are presented in HosseiniArani et al. (2024).

The expected sensitivity of space-based Q-ACCs based on state-of-the-art technology is on the order of 5×10^{-10} m/s^2/$\sqrt{\text{Hz}}$. To have comparable accuracy with a GRACE-like accelerometer, we consider an optimized version of the state-of-the-art scenario discussed in HosseiniArani et al. (2024) (see Table 1), and we study its hybridization with a GRACE-like E-ACC.

In another scenario, we consider a highly improved Q-ACC, which we expect to be achieved in the next 5–10 years, equivalent to the near-future scenario given in HosseiniArani et al. (2024), and we study its hybridization of an improved E-ACC. Figure 1 shows the expected performance of the quantum and electrostatic sensors for the two scenarios mentioned.

Note that in all our scenarios, we assume a three-axis E-ACC combined with a one-axis Q-ACC with its sensitivity axis aligned to the along-track direction of the satellite. The motivation for keeping the sensitivity axis along-track is that the non-gravitational acceleration in flight path is the most critical component for a GRACE-like mission, that is, the acceleration of the satellite along this direction directly affects the determination of the gravity field.

Misalignment between Q-ACC and E-ACC typically ranges from tens to about 100 μrad pre-launch, due to precision limitations in mechanical assembly and ground calibration (Zahzam, Christophe, Bresson, et al., 2022). Laboratory experiments have demonstrated that careful pre-launch calibration alone can ensure alignment accuracies down to a few microradians (Templier et al., 2022). In addition, structural and thermal effects may cause dynamic variations in misalignment during a mission—such as periodic fluctuations linked to orbital thermal cycling, structural distortions, or mechanical vibrations (Migliaccio et al., 2022). This paper assumes that in-flight calibration methods effectively reduce these misalignments to negligible levels, and perfect alignment between quantum and conventional sensors is assumed after initial calibration.

Moreover, the impact of the misalignment on the performance of the hybrid accelerometer mainly depends on the orientation of the satellite during the trajectory. For constant orientation with respect to the non-gravitational forces, the effect of residual misalignment can be compensated by the acceleration bias estimate

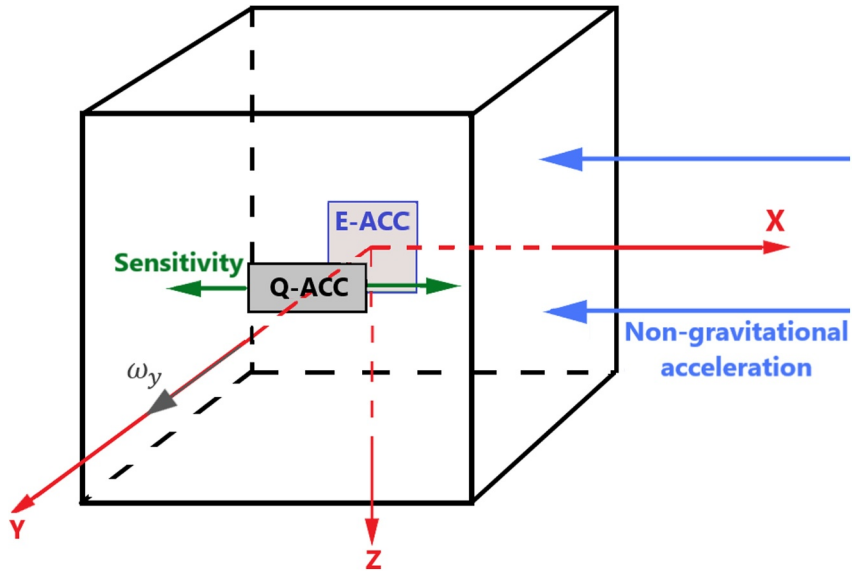

Figure 2. Positioning of the quantum accelerometer (Q-ACC) inside the satellite frame considering that the electrostatic accelerometer is in the center of mass. The Q-ACC accelerometer is placed on the cross-track axis of the satellite. The sensitivity axis of the Q-ACC is parallel to the along-track axis of the satellite.

(Tennstedt, 2025). For future implementations, the extended Kalman Filter (EKF) state vector might be augmented by the misalignment, potentially allowing an online calibration.

2.3. Effect of Satellite Rotation

When the quantum sensor is in a rotating body frame, for example, a nadir-pointing satellite, based on Equation 3, there will be an additional phase shift caused by the Coriolis and centrifugal accelerations. The largest contribution of this rotation to the phase shift of the atom interferometer arises from the Coriolis acceleration induced by the atomic velocity in the radial direction (Lan et al., 2012; Lévèque et al., 2021). Also, centrifugal and Euler accelerations lead to additional terms. In our previous study of the hybrid accelerometer (HosseiniArani et al., 2022), we assumed to have a perfect knowledge of the rotational accelerations, and therefore, only the measurements of linear accelerations by an E-ACC were considered as the measurements of conventional IMU. In this study, we consider the whole rotational effect. To do so, we first model the angular dynamics of the satellite and an attitude control system for a GRACE-like satellite. Then, we model the measurement of gyroscopes by adding white noise to the true angular velocities. Finally, we model the effect of the rotation on the measurements of the Q-ACC. If the rotation of the satellite is not properly compensated, the solution will degrade considerably. Therefore, several approaches are proposed to physically compensate the effect of the rotation (see Beaufils et al., 2023; Zahzam, Christophe, Lebat, et al., 2022).

The positioning of the classical and Q-ACCs within the satellite frame, as well as the rotational compensation method that is used against the satellite's rotation around the cross-track axis, have a considerable impact on the accuracy of the Q-ACC. For a comparison of different sensor positioning and rotation compensation methods, we refer the reader to HosseiniArani et al. (2024). Here, we consider only one of the optimal situations for satellite gravity missions, as detailed therein, in which the classical sensor is placed at the center of mass of the satellite and the quantum sensor is placed beside it on the cross-track axis of the satellite (see Figure 2). Note that the sensitivity axis of the quantum sensor is still in the along-track direction, so we only measure the accelerations in this direction which is the main direction of interest for GRACE-like missions. This configuration minimizes the impact of centrifugal accelerations caused by the primary rotation around the cross-track axis by reducing the lever arm. The two main rotation compensation methods use active counter-rotating Raman mirrors and counter-rotating the whole quantum sensor against the satellite rotation around the cross-track axis. The implementation of these methods in our simulations is described in HosseiniArani et al. (2024). Here, we use the former method for our first scenario and the latter for our second scenario. We then study the hybridization in both scenarios. The phase shift due to the satellite rotation can be calculated based on Beaufils et al. (2023):

Table 2
Different Signal Contributions to the Phase Shift

Contributions to the phase shift	Size (rad)	Fractional size
Non-Gravitational Acceleration	19.97	1
Uncompensated Rotation	8.6×10^{-3}	4.3×10^{-4}
Self-Gravity	4.8×10^{-5}	2.4×10^{-6}
Gravity Gradient (V_{xx})	3.1×10^{-6} [a]	1.5×10^{-7}

[a]This number is calculated for the interrogation time ($2T$) of 10 s; if the interrogation time is considered to be 5 s, then this phase shift contribution would be 3.87×10^{-7} rad.

$$\Delta\Phi = 2k_{\text{eff}}T^2\left[a_x + 2v_{z0}(\Omega_y + \Omega_M) - x_0{\Omega_y}^2 + (x_0 - x_M)\left({\Omega_M}^2 + (\Omega_M - \Omega_I)^2\right)\right] \quad (3)$$

where x_0 is the initial distance of atoms to the satellite center of mass, x_M is the distance of the center of rotation of the mirror to the satellite center of mass, Ω_y is the angular velocity of the satellite around the cross-track axis with respect to the inertial frame, Ω_M and Ω_I are the angular velocities of the mirror and incoming laser beam, with respect to the satellite body-fixed frame, and v_{z0} is the initial velocity of atoms in the radial direction of the satellite body frame. In the case of rotation compensation using an active counter-rotating mirror, a high-performance on-board gyroscope can be used to measure the satellite rotation at each instant in time and cancel its contribution to the phase shift by an active Raman mirror rotating against the rotation rate of the satellite (Lan et al., 2012; Migliaccio et al., 2019). In this scenario, the incoming laser is assumed to be fixed in the body frame of the satellite and has a rotation rate identical to that of the satellite ($\Omega_I = 0$ and $\Omega_M = -\Omega_y$). We also assume that the center of rotation of the mirror is in the same place as the center of mass of the satellite ($x_M = 0$) on the along-track axis. Therefore, Equation 3 can be simplified as follows

$$\Delta\Phi = 2k_{\text{eff}}T^2\left[a_x + x_0{\Omega_y}^2\right]. \quad (4)$$

The term $x_0{\Omega_y}^2$ is the remaining term after compensation of rotation by a counter-rotating Raman mirror. In the case of rotation compensation by counter-rotating the entire sensor, this remaining term will also be removed from the phase shift equation. However, technical difficulties might arise in the realization of this method. In both scenarios, the effectiveness of rotation compensation will be highly dependent on our knowledge of the rotation rates. The details of these formulations are discussed in HosseiniArani et al. (2024).

In space-based atom interferometry, controlling the orientation of the quantum sensor is essential for suppressing systematic effects and noise. By changing the sensor's orientation, it becomes possible to discriminate true inertial signals from systematic effects (Geiger et al., 2011). Any uncertainty in the sensitivity axis of the sensors will result in an error in the measured acceleration. Table 1 presents the pointing error requirements for the mission, ensuring that the quantum sensor achieves its expected performance.

2.4. Gravity Gradient and Self-Gravity

As shown in Figure 2, the quantum sensor is assumed to be displaced from the center of mass of the satellite, which leads to an additional phase shift due to the gravity gradient. However, since the sensitivity axis of the quantum sensor is assumed to be in the along-track direction, only the gravity gradient g_{xx} in the along-track direction results in an additional phase shift. Our simulations show this effect has a small value and, therefore, can be neglected (see Table 2). Self-gravity is the gravitational pull of the spacecraft's mass on the free-falling atoms. Depending on the position of the quantum sensor and the direction of its sensitivity axis, the self-gravity effect can also result in an additional phase shift. Our simulations show that if the quantum sensor is placed on the along-track axis, a 20 cm displacement can cause a considerable phase shift in the order of 0.27 rad. However, by having knowledge of the satellite mass and the displacement, this phase shift can be calculated and removed from the measurements. Moreover, if the quantum sensor is placed on the cross-track axis of the satellite while its sensitivity axis is still in the along-track direction (similar to the situation in Figure 2), the self-gravity effect would be minimal. Table 2 shows the self-gravity phase shift in this scenario, which is around two orders of magnitude smaller than the total root mean square (RMS) phase noise of the sensor and can be neglected. The other self gravity contribution is due to the closest structures to the atom clouds. To overcome this issue compensating masses are usually needed (Armano et al., 2016).

In addition to the above-mentioned signals, there are higher-order contributions that couple these inertial forces, particularly with gravity gradients. However, because of the smaller contributions of these additional terms and since the sensitivity axis of the Q-ACC is aligned in the along-track direction of the satellite and then the gravity gradient in the along-track direction is considerably smaller than in the radial direction, the additional phase shift

gets relatively small values. Table 2 compares the contributions of the non-gravitational accelerations, rotation, gravity gradient and self-gravity effects on the total phase shift of Q-ACCs. Given the comparatively small values of the phase shift due to the gravity gradient and self-gravity, we ignore these terms in our modeling and take into account only the rotation terms.

2.5. Extended Kalman Filter

Our EKF seeks to combine the measurements of the two accelerometers while simultaneously using the measurements of the E-ACC to solve phase ambiguities of the Q-ACC. In essence, the phase ambiguity solution is realized by a prediction of the Q-ACC observation with the data of the E-ACC and gyroscope, using a model according to Equation 3, in which the acceleration a_x is assessed by the E-ACC model from Equation 2.

The predicted observation of the Q-ACC h_i at a discrete time indicated by index i is produced by the predicted phase shift $\Delta\Phi_i$. It reads

$$h_i(\Delta\Phi_i) = A\cos\left(\Delta\Phi_i + \phi_{L,i}\right) + \nu. \tag{5}$$

The fringe parameters A and ν are each assumed to have a value of 0.5. It is further anticipated that the laser phase $\phi_{L,i}$ is steered, such that the sum of $\Delta\Phi_i + \phi_{L,i}$ equals $\pi/2$. An estimate $\hat{B}_i$ of the E-ACC is then obtained based on the difference of this prediction and the actual Q-ACC observation $p_{CAI,i}$ via

$$\hat{B}_i = -K_i\left(p_{CAI,i} - h_i(\Delta\Phi_i)\right). \tag{6}$$

This innovation $p_{CAI,i} - h_i(\Delta\Phi_i)$ is weighted by the Kalman gain K_i,

$$K_i = \frac{P_i^- H_i}{R_i + H_i^2 P_i^-}, \tag{7}$$

which itself is related to the *predicted* state variance P_i^-, the observation variance R_i and the observation sensitivity H_i,

$$H_i = \frac{\partial h_i}{\partial B} = 2k_{\text{eff}}T^2, \tag{8}$$

of the model to the bias. The state variance P_i^- is predicted before the evaluation of Equation 7 via

$$P_i^- = P_{i-1}^+ + Q_i. \tag{9}$$

here, Q_i is the process noise which corresponds to the uncertainty of the E-ACC. P_{i-1}^+ is the *filtered* variance of the prior update, which is defined by

$$P_i^+ = (1 - K_i H_i)^2 P_i^- + K_i^2 R_i. \tag{10}$$

This method was already applied in HosseiniArani et al. (2022). Since Equation 3 does not yield any additional terms including a_x, and thus no additional sensitivities to B, no major adaptions of the settings are necessary. However, in the presence of rotation, the determination of the Q-ACC phase ambiguity could be affected in some cases.

The effect of satellite rotation on the measurements of the Q-ACC is discussed in Section 2.3. In our Kalman filtering strategy, we use the phase shift equivalent to the acceleration measured by the E-ACC to determine the phase ambiguity of the quantum sensor. Since the rotation can cause an additional phase shift, and because of the noisy nature of the measurements of rotation rates by gyroscopes, there will be an additional error in the determination of the quantum sensor phase ambiguity with respect to the situation in which no rotational noise is assumed. For additional insight into the general EKF framework, the reader is referred to Tennstedt et al. (2023).

2.6. Recovery of the Gravity Field

We investigate the effect of combined accelerometers in the recovery of the gravity field. For this part, a closed-loop simulation procedure was used (Kupriyanov, Reis, Knabe, et al., 2024) in which, at first, the orbital simulations were carried out in XHPS software (Wöske et al., 2019). Then, computed satellite positions were utilized in the gravity field recovery software that follows the procedure introduced by (Wu, 2016). And finally, retrieved gravity field models were compared with the reference one (EIGEN-6C4) by calculating residuals and plotting them in the spatial (as global maps) and spectral (as degree RMS graphs) domains.

The primary aim of this study is to isolate and analyze the impact of incorporating a quantum sensor on enhancing gravity field recovery. Therefore, in our simulation, we first neglect the contributions of temporal aliasing and insufficient background modeling to gravity field recovery.

We acknowledge, however, that realizing the full potential of Q-ACCs in future gravity missions will require concurrent improvements in other areas, particularly in minimizing errors from background modeling. Background modeling refers to the modeling of ocean tides and non-tidal mass variability in the atmosphere and ocean. Addressing these aspects in details will be the focus of future research. However, to mitigate any potential ambiguities in our findings, we have included an additional scenario in Section 3.5. In this scenario, we evaluate the improvement achieved by integrating a Q-ACC, while also factoring in the noise introduced by insufficient background modeling. A brief description of this scenario and the corresponding results are provided.

We point out that future improvements in de-aliasing products, like the Atmosphere and Ocean non-tidal De-aliasing Level-1B (AOD1B) product (Shihora et al., 2022), can be applied in post-processing to the benefit of previous and existing satellite gravimetry missions, however, improvements in sensor technology can not be applied in retrospect. The error due to the imperfect modeling in the AOD1B R07 can be estimated by the AOe07 data product (Shihora et al., 2024).

3. Results

3.1. Performance of the Hybrid Accelerometer for the State-of-the-Art Scenario

We investigate the efficiency of the Kalman filter in three different scenarios. In the first scenario, we consider an optimized version of the state-of-the-art Q-ACC based on HosseiniArani et al. (2024) and the characteristics described in Table 1 in a hybrid combination with a state-of-the-art E-ACC and similar to the GRACE-FO accelerometer as discussed in Section 2. Assumptions for the noise of the accelerometers are shown in Figure 1.

In Section 2.5, we described how we estimate the bias of the E-ACC $\left(\hat{B}\right)$ based on the difference of the prediction and the actual Q-ACC observation. Figure 3 shows the estimated bias as an output of the EKF compared to the true E-ACC bias (true non-gravitational signal minus the measurements of the E-ACC).

3.2. Hybridization for the Near-Future Scenario

New E-ACCs have been demonstrated and tested that can achieve considerably better sensitivity at higher frequencies (Dávila Álvarez et al., 2022). At the same time, with the ongoing advances in atom interferometry, improved Q-ACCs are also expected to be realized. We have summarized the impact of key parameters, such as atomic number and temperature, laser system, rotation sensing and mitigation schemes, and their potential for improvement on instrument performance in (HosseiniArani et al., 2024). Therefore, in our second scenario, we consider one order of magnitude improvement in the noise of the E-ACC. To have a meaningful combination, we assume a near-future Q-ACC as described in HosseiniArani et al. (2024) reaching a sensitivity of the level of 1×10^{-11} m/s^2/$\sqrt{\text{Hz}}$ (see Figure 1 for the accelerometer noise assumptions).

Figure 4 compares the amplitude spectral densities of the quantum and electrostatic accelerometers with the filter solution for both above-mentioned scenarios, where the modeled non-gravitational accelerations are removed. The filter output has gained the stability of Q-ACC measurements at lower frequencies and benefited from the capabilities of the E-ACC at higher frequencies.

HosseiniArani et al. (2024) displays how the rotational phase shift can considerably reduce the interferometer contrast if not properly compensated. It also discusses the impact of different rotation compensation methods on the observation of the quantum sensor. In Section 2.5, we discussed the additional error that could affect the

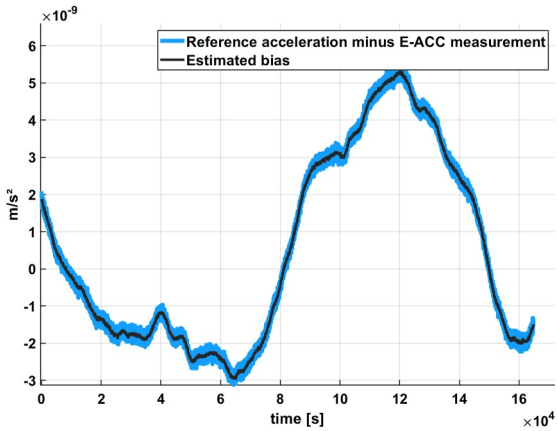

Figure 3. Bias estimation, using the hybrid accelerometer concept for the state-of-the-art scenario; Blue: The difference between the true non-gravitational acceleration signal and the measurements of E-ACC; Black: Estimated bias using extended Kalman filtering.

determination of the quantum sensor ambiguity and the convergence of the Kalman filter. This error is due to the noise on the measurements of the rotation rate compared to the situation where we assume to have perfect knowledge of the rotation. If a proper rotation compensation method is used (based on HosseiniArani et al., 2024), and the rotational rates are known with the expected accuracy (see Table 1), this additional error will not prevent from properly removing the phase ambiguity, nor affect the convergence of the filter.

3.3. Hybridization at Lower Altitudes

In our third scenario, we consider the same accelerometers that were discussed in our first scenario. However, this time, we assume to have GRACE-like satellites at a lower altitude of 300 km. We want to see if the increase in the amplitude of the non-gravitational and rotational accelerations would have any impact on the filter output.

Figure 5 compares the recovered bias with the true simulated bias of the E-ACC for our third scenario. In this scenario, the filter experiences initial high-amplitude fluctuations in the recovery of the bias, but apart from that, no other meaningful difference in the behavior of the filter is observed. These initial fluctuations are a direct result of the initial wobbling of the satellite in our simulations. They can destroy the filter solution and result in an incorrect bias recovery. However, starting the filter with some delay after the start of the simulation avoids the fluctuations and leads to a filter noise similar to what is shown in dark green in Figure 4.

3.4. Performance in the Recovery of the Gravity Field

The non-gravitational accelerations in the along-track direction of a GRACE-like mission directly affect the determination of the gravity field. Therefore, by adding a Q-ACC in the along-track direction, we aim for a better determination of the gravity field. Here, we investigate the performance of the combined classical and Q-ACCs for recovering the Earth's gravity field.

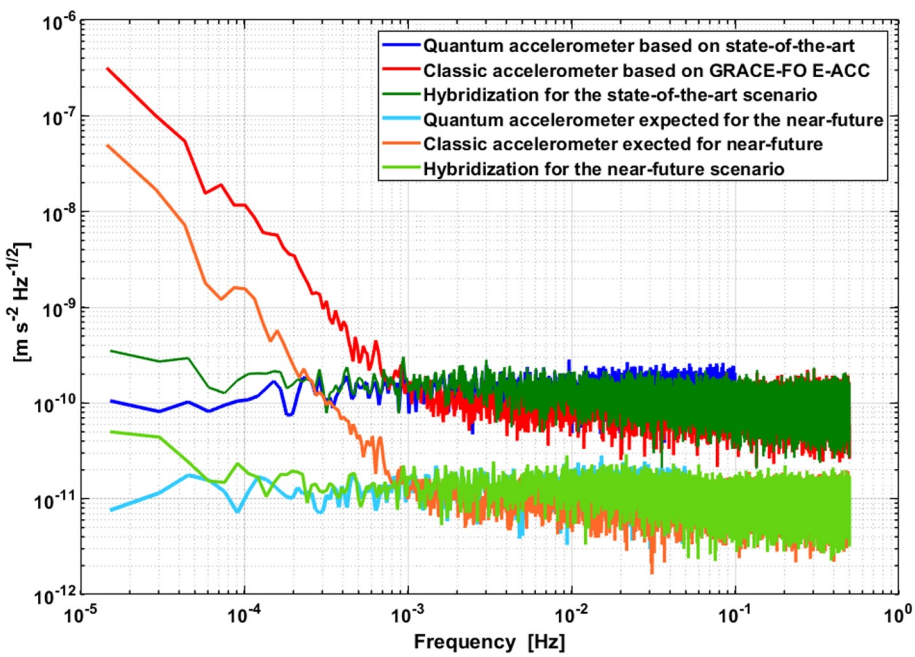

Figure 4. Hybridization of classical and quantum accelerometers for the state-of-the-art and near-future scenarios; spectral representation of the solutions in terms of amplitude spectral density for Q-ACC (dark and light blue), classical accelerometers (red and orange), and the Kalman-filter-based hybridization (dark and light green).

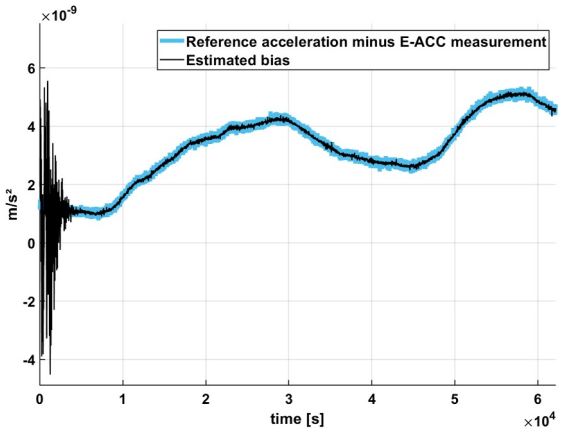

Figure 5. Bias estimation, using the hybrid accelerometer concept with the satellite pair being at the altitude of 300 km; Blue: The difference between the true non-gravitational acceleration signal and the measurements of the E-ACC; Black: Estimated bias using extended Kalman filtering.

Figure 6 shows the degree RMS of the coefficient differences between reference and recovered gravity field in units of geoid height. One can see one and two orders of improvement in geoid height by replacing the classical accelerometer with the state-of-the-art hybrid and near-future hybrid accelerometers, respectively. Figures 7 and 8 compare the global map of the residuals and the spherical harmonic error spectrum of the recovered gravity fields retrieved until degree and order (d/o) 180 for the state-of-the-art and near-future hybrid accelerometers concepts. The spherical harmonic error is displayed in a triangle plot showing the unitless numerical differences of the recovered gravity field coefficients with respect to the coefficients of the input gravity field (EIGEN-6C4). The x-axis represents the order of the gravity field expansion with the sine coefficients S_{lm} to the left and the cosine coefficients C_{lm} to the right of the plot. The y-axis shows the degree of the gravity field expansion. The colorbar of the triangle plots is presented in logarithmic scale limited from 1×10^{-10} to 10^{-14}.

Global maps are shown before post-processing and filtering, illustrating the improvements achieved by adding the Q-ACC and introducing the hybrid concept in the state-of-the-art scenario (see Figure 7b). Moreover, the produced global gravity field maps show a considerable reduction of the instrumental contribution to the striping effect after introducing the hybrid accelerometers (see Figure 8a). The possibilities and challenges of having an improved Q-ACC for the near future are discussed in HosseiniArani et al. (2024). Finally, Figure 8b displays the improvements in the gravity field that can be achieved by adding the LRI 2030 to the near future-hybrid accelerometer concept.

3.5. Contribution of Temporal Aliasing and Insufficient Background Modeling

In the previous sections, we neglected the effects of temporal aliasing and insufficient background modeling on gravity field recovery to focus on the benefits of adding a Q-ACC. In this Section, however, we consider scenarios that account the noise due to insufficient background modeling. We specifically examine errors in background models by focusing on ocean-tide discrepancies between the monthly averaged EOT11a (Savcenko & Bosch, 2012) and FES2014b (Lyard et al., 2021) releases. Additionally, we analyze atmospheric-ocean de-aliasing data from AOe07 (Shihora et al., 2024), which is interpolated to each time step.

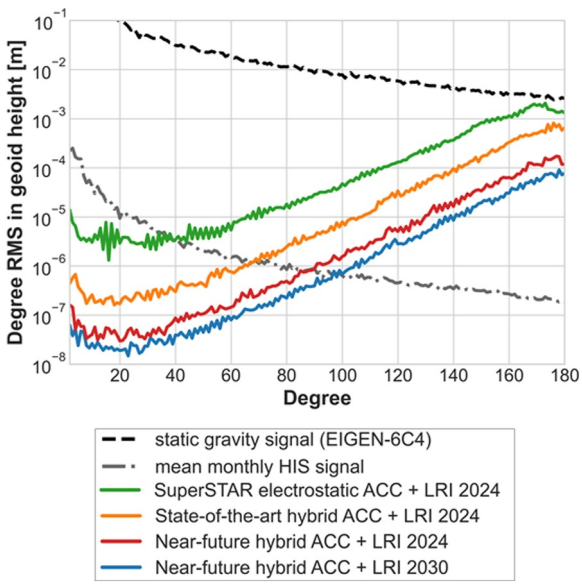

Figure 6. Degree root mean square of the spherical harmonic coefficient differences (true errors) plotted in geoid height [m]; the effects of temporal aliasing and insufficient background modeling are neglected.

Figure 9 shows the degree RMS of the spherical harmonic coefficient differences for the following ll-SST cases including time-variable background modeling errors: (a) the current GRACE-FO simulated monthly solutions, and (b) the scenario with the state-of-the-art hybrid accelerometers onboard the mission. In spite of the fact that background modeling error overwhelmingly dominates the instrument errors, a certain improvement in gravity field recovery can be noticed using the hybrid inertial sensor starting from spherical harmonic degree 10.

We conclude that a certain improvement in gravity field recovery can be observed in the presence of background modeling. However, for future gravity missions aiming to fully leverage advanced Q-ACCs, parallel advancements will be required. Specifically, enhancements in the ranging instrument (cf. Figure 1) and efforts to minimize temporal aliasing—such as by increasing the accuracy of background modeling—will be crucial. The latest atmosphere and ocean dealiasing product AOD1B RL07 (Shihora et al., 2022) uses the current ERA5 model (Hersbach et al., 2020) as well as the MPIOM general ocean circulation model (Jungclaus et al., 2013). The largest potential for the reduction of temporal aliasing is in the improvement of the ocean model. The AOe07 data product (Shihora et al., 2024), which provides an uncertainty estimation for AOD1B RL07, is an additional improvement in the methods of

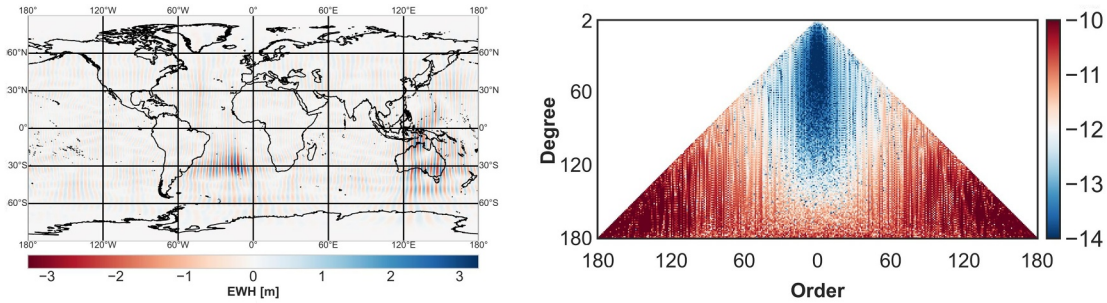

(a) SuperSTAR E-ACC + KBR

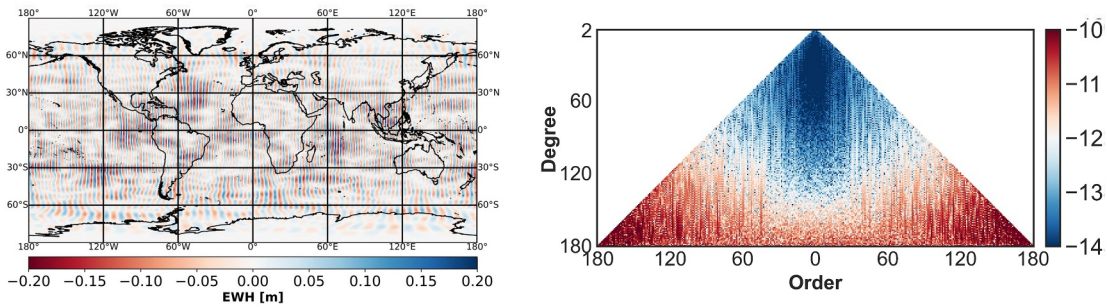

(b) State-of-the-art Hybrid ACC + LRI 2024

Figure 7. Comparison of the spatial distribution of the residuals plotted on the global maps of the recovered gravity field w.r.t. reference EIGEN-6C4 (without post-processing and filtering) from the GRACE mission (a) and the state-of-the-art hybrid accelerometers concept (b). Global maps plotted til d/o 90 (plots on the left); spherical harmonic error in log scale of the coefficient differences plotted til d/o 180 (plots on the right).

gravity field recovery from GRACE (-FO) observations to reduce temporal aliasing as well as to create more realistic satellite gravimetry mission simulations.

We point out that upcoming double pair constellations like MAGIC (Heller-Kaikov et al., 2023) will also reduce the temporal aliasing error thereby requiring less signal processing (e.g. smaller filter radius) keeping smaller details in the signals unaffected. Lastly, evaluating large constellations which span the whole globe on several orbital planes, for example Starlink (Liu et al., 2024) or Europe's IRIS^2 (EU Agency for the Space Programme, 2024), can also add to the reduction of temporal aliasing. The European constellation is set to be operational by 2030 with satellites in low and medium Earth orbit. Such large satellites constellations, which cover the whole planet more or less instantaneous, can be used to process daily or higher frequency gravity field solutions with a lower degree and order compared to typical monthly gravity fields. However, these low resolution gravity fields are sufficient to measure variations in the atmosphere and ocean with a large geographical extent, which contribute most to the temporal aliasing effect. Potentially, the larger constituents of ocean tides can be recovered. This is the topic of future work.

One of the first steps for the realization of a Q-ACC onboard a gravimetry mission is the CARIOQA Quantum Pathfinder mission (Lévèque et al., 2022) which is funded by the European Union with a desired launch in 2030. The aim of this mission is the demonstration of a Q-ACC in space to raise the technology readiness level of components necessary for a later quantum space gravimetry mission. Considering this timeline, the aforementioned improvements in ranging technology, background modeling and potential augmentation by other satellite constellations will have progressed beyond the current state of the art to fully utilize the improved accelerometer technology.

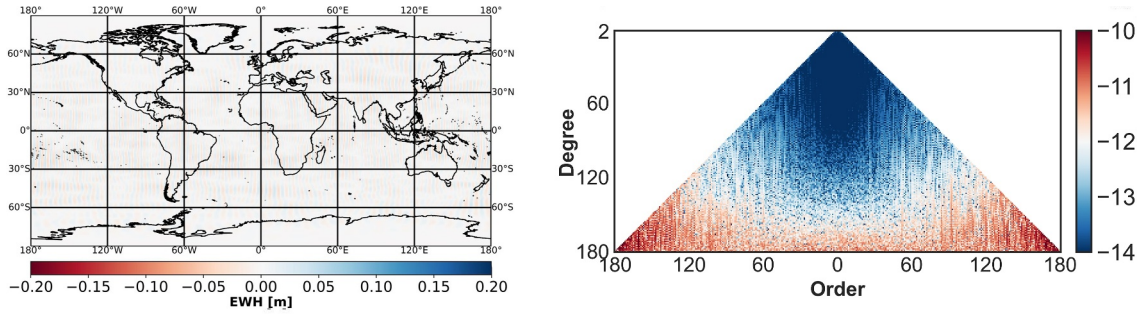

(a) Near-future Hybrid ACC + LRI 2024

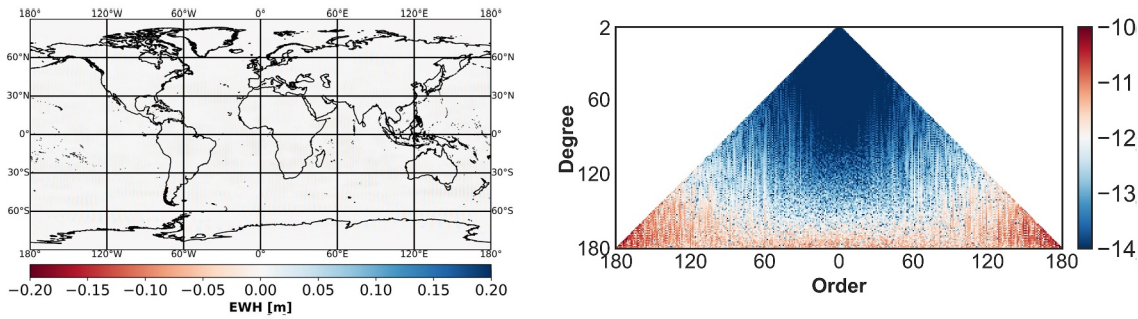

(b) Near-future Hybrid ACC + LRI 2030

Figure 8. Comparison of the recovered gravity fields retrieved til d/o 180 (without post-processing and filtering) from the near-future hybrid accelerometers concepts w. r.t. EIGEN 6C4. Global maps plotted til d/o 90 (plots on the left); spherical harmonic error in log scale of the coefficient differences plotted til d/o 180 (plots on the right).

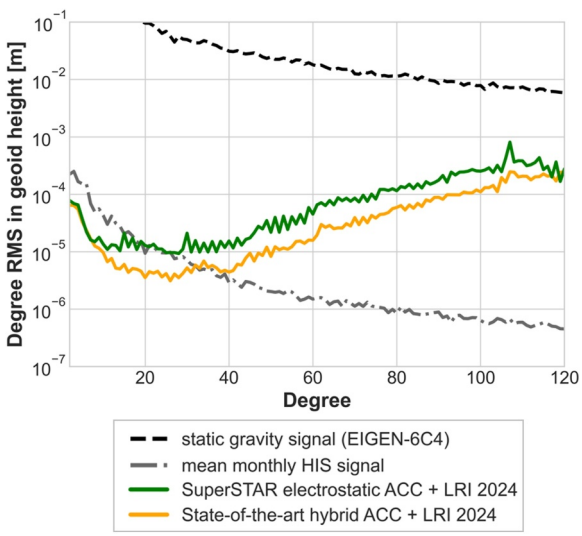

Figure 9. Degree root mean square of the spherical harmonic coefficient differences (true errors) plotted in geoid height [m] from ll-SST simulations including time-variable background modeling errors (OT: difference between EOT11a and FES2014b; AOD: AOe07, interpolated to 5 s); Green: simulated monthly solution considering the current instruments of the GRACE-FO mission; Orange: simulated solution when using a state-of-the-art hybrid accelerometer in a GRACE-like mission.

4. Conclusions

We considered an advanced Kalman-filter-based hybridization of electrostatic and Q-ACCs by implementing a comprehensive noise model for satellite-based quantum sensors and considering the full impact of satellite rotation on the sensor's measurements. We studied the hybridization of state-of-the-art and near-future classical and quantum sensors and quantified their impacts on the performance of future satellite gravity missions. The filter converges in all scenarios. The solution benefits from the performances of the E-ACC measurements at higher frequencies, together with the high stability of Q-ACC measurements at lower frequencies Thus the capability to online estimate and correct biases of the E-ACC. This holds true, even in presence of rotational effects. When a proper rotation compensation method is applied, the additional noise due to the rotation rate does not prevent the convergence of the filter.

Our results indicate that implementing a hybrid accelerometer on-board a future gravity mission will improve the gravity field solution by one to two orders in both, lower and higher degrees. The global gravity field maps show considerable improvement in reducing the instrumental contribution to the striping effect by introducing hybrid accelerometers. Note that while adding a Q-ACC shows great potential for improving gravity field recovery, its benefits are partially diminished by errors from current insufficient background modeling, particularly in ocean-tide and atmospheric-ocean data. Our analysis indicates that, without significant advancements in background modeling accuracy, the improvements from hybrid accelerometers will remain limited.

Future gravity missions must address these modeling challenges to fully realize the advantages of quantum sensor technology. We note that upcoming double-pair constellations like MAGIC can also reduce temporal aliasing errors, and large global constellations such as Starlink or IRIS^2 may also help address this issue. Beyond satellite gravimetry missions, quantum and hybrid inertial sensors also hold promise for a range of additional space applications, such as planetary geodesy and space navigation. These extended applications will be the focus of future investigations.

Data Availability Statement

The data used in this study for simulating the satellite orbit, the noise time series of the hybrid accelerometers, and the coefficients of the recovered gravity fields are available from (HosseiniArani et al., 2025).

Acknowledgments
This work is supported by the Deutsche Forschungsgemeinschaft (DFG, German Research Foundation) Collaborative Research Center 1464 "TerraQ"—434617780 and Germany's Excellence Strategy—EXC-2123 "QuantumFrontiers"—390837967, and by the European Union's Horizon Europe research and innovation programme under grant agreement No 101081775 (CARIOQA-PMP project). This study is also partially supported by SpaceQNav project funded by the Federal Ministry for Economic Affairs and Climate Action (BMWK), Project 50NA2310 A. QB and FP acknowledge the support of a government grant managed by the Agence Nationale de la Recherche under the Plan France 2030, with the reference "ANR-22-PETQ-0005." B.T. acknowledges support from the Federal Ministry for Economic Affairs and Climate Action (BMWK), Project 50NA2106. J.M. and A.K. acknowledge support by Deutsches Zentrum für Luft- und Raumfahrt e.V (DLR). for the project Q-BAGS. Open Access funding enabled and organized by Projekt DEAL.

References

Abich, K., Abramovici, A., Amparan, B., Baatzsch, A., Okihiro, B. B., Barr, D. C., et al. (2019). In-orbit performance of the GRACE follow-on laser ranging interferometer. *Physical Review Letters*, *123*(3), 031101. https://doi.org/10.1103/PhysRevLett.123.031101

Altin, P. A., Johnsson, M. T., Negnevitsky, V., Dennis, G. R., Anderson, R., Szigeti, S. S., et al. (2013). Precision atomic gravimeter based on Bragg diffraction. *New Journal of Physics*, *15*(2), 023009. https://doi.org/10.1088/1367-2630/15/2/023009

Armano, M., Audley, H., Baird, J., Bassan, M., Binetruy, P., Born, M., et al. (2016). Sub-femto-g free fall for space-based gravitational wave observatories: Lisa pathfinder results. *Physical Review Letters*, *116*(23), 231101. https://doi.org/10.1103/PhysRevLett.116.231101

Asenbaum, P., Overstreet, C., Kim, M., Curti, J., & Kasevich, M. A. (2020). Atom-interferometric test of the equivalence principle at the 10^{-12} level. *Physical Review Letters*, *125*(19), 191101. https://doi.org/10.1103/PhysRevLett.125.191101

Beaufils, Q., Lefebve, J., Baptista, J. G., Piccon, R., Cambier, V., Sidorenkov, L. A., et al. (2023). Rotation related systematic effects in a cold atom interferometer onboard a nadir pointing satellite. *NPJ microgravity*, *9*(1), 53. https://doi.org/10.1038/s41526-023-00297-w

Cheinet, P., Canuel, B., Pereira Dos Santos, F., Gauguet, A., Yver-Leduc, F., & Landragin, A. (2008). Measurement of the sensitivity function in a time-domain atomic interferometer. *IEEE Transactions on Instrumentation and Measurement*, *57*(6), 1141–1148. https://doi.org/10.1109/TIM.2007.915148

Chen, J., Cazenave, A., Dahle, C., Llovel, W., Panet, I., Pfeffer, J., & Moreira, L. (2022). Applications and challenges of GRACE and GRACE Follow-On satellite gravimetry. *Surveys in Geophysics*, *43*(1), 305–345. https://doi.org/10.1007/s10712-021-09685-x

Christophe, B., Boulanger, D., Foulon, B., Huynh, P. A., Lebat, V., Liorzou, F., & Perrot, E. (2015). A new generation of ultra-sensitive electrostatic accelerometers for GRACE Follow-On and towards the next generation gravity missions. *Acta Astronautica*, *117*, 1–7. https://doi.org/10.1016/j.actaastro.2015.06.021

Christophe, B., Foulon, B., Liorzou, F., Lebat, V., Boulanger, D., Huynh, P.-A., et al. (2018). Status of development of the future accelerometers for next generation gravity missions. In J. T. Freymueller & L. Sánchez (Eds.), *International Symposium on Advancing Geodesy in a Changing World* (Vol. 149, pp. 85–89). Springer International Publishing. https://doi.org/10.1007/1345_2018_42

Christophe, B., Guidotti, P.-Y., Reynaud, S., Foulon, B., Josselin, O., Touboul, M., & Izzo, D. (2009). Odyssey: A test of the equivalence principle in space. *Classical and Quantum Gravity*, *29*(18), 184013. https://doi.org/10.1088/0264-9381/29/18/184013

Dávila Álvarez, A., Knudtson, A., Patel, U., Gleason, J., Hollis, H., Sanjuan, J., et al. (2022). A simplified gravitational reference sensor for satellite geodesy. *Journal of Geodesy*, *96*(10), 70. https://doi.org/10.1007/s00190-022-01659-0

Deppner, C., Herr, W., Cornelius, M., Stromberger, P., Sternke, T., Grzeschik, C., et al. (2021). Collective-mode enhanced matter-wave optics. *Physical Review Letters*, *127*(10), 100401. https://doi.org/10.1103/PhysRevLett.127.100401

EU Agency for the Space Programme. (2024). IRIS^2 (infrastructure for resilience, interconnectivity and security by satellite). Retrieved from https://www.euspa.europa.eu/eu-space-programme/secure-satcom/iris2

Flury, J., Bettadpur, S., & Tapley, B. D. (2008). Precise accelerometry onboard the GRACE gravity field satellite mission. *Advances in Space Research*, *42*(8), 1414–1423. https://doi.org/10.1016/j.asr.2008.05.004

Flury, J., & Rummel, R. (2005). Future satellite gravimetry for geodesy. *Earth, Moon, and Planets*, *94*(1–2), 13–29. https://doi.org/10.1007/s11038-005-3768-7

Freier, C., Hauth, M., Schkolnik, V., Leykauf, B., Schilling, M., Wziontek, H., et al. (2016). Mobile quantum gravity sensor with unprecedented stability. *Journal of Physics: Conference Series*, *723*, 012050. https://doi.org/10.1088/1742-6596/723/1/012050

Geiger, R., Landragin, A., Merlet, S., & Pereira Dos Santos, F. (2020). High-accuracy inertial measurements with cold-atom sensors. *AVS Quantum Science*, *2*, 024702. https://doi.org/10.1116/5.0009093

Geiger, R., Ménoret, V., Stern, G., Zahzam, N., Cheinet, P., Battelier, B., et al. (2011). Detecting inertial effects with airborne matter-wave interferometry. *Nature Communications*, *2*(1), 474. https://doi.org/10.1038/ncomms1479

Haagmans, R., Siemes, C., Massotti, L., Carraz, O., & Silvestrin, P. (2020). ESA's next-generation gravity mission concepts. *Rendiconti Lincei. Scienze Fisiche e Naturali*, *31*(S1), 15–25. https://doi.org/10.1007/s12210-020-00875-0

Hartmann, S., Abend, S., Schubert, C., Gersemann, M., Ahlers, H., Herr, W., et al. (2020). Operating an atom interferometer beyond its coherence time. *Physical Review A*, *101*(5), 053610. https://doi.org/10.1103/PhysRevA.101.053610

Heller-Kaikov, B., Pail, R., & Daras, I. (2023). Mission design aspects for the mass change and geoscience international constellation (MAGIC). *Geophysical Journal International*, *235*(1), 718–735. https://doi.org/10.1093/gji/ggad266

Hersbach, H., Bell, B., Berrisford, P., Hirahara, S., Horányi, A., Muñoz-Sabater, J., et al. (2020). The ERA5 global reanalysis. *Quarterly Journal of the Royal Meteorological Society*, *146*(730), 1999–2049. https://doi.org/10.1002/qj.3803

HosseiniArani, A., Schilling, M., Beaufils, Q., Knabe, A., Tennstedt, B., Kupriyanov, A., et al. (2024). Advances in atom interferometry and their impacts on the performance of quantum accelerometers on-board future satellite gravity missions. *Advances in Space Research*, *74*(7), 3186–3200. https://doi.org/10.1016/j.asr.2024.06.055

HosseiniArani, A., Schilling, M., Tennstedt, B., Kupriyanov, A., Beaufils, Q., Knabe, A., et al. (2025). Combined-accelerometers-for-satellite-gravity-missions-study [Dataset]. *LUIS*. https://doi.org/10.25835/w85ssyb3

HosseiniArani, A., Tennstedt, B., Schilling, M., Knabe, A., Wu, H., Schön, S., & Müller, J. (2022). Kalman-filter based hybridization of classic and cold atom interferometry accelerometers for future satellite gravity missions. In J. Freymueller & L. Sanchez (Eds.), *Geodesy for a Sustainable Earth* (Vol. 154, pp. 221–231). Springer. https://doi.org/10.1007/1345_2022_172

Humphrey, V., Rodell, M., & Eicker, A. (2023). Using satellite-based terrestrial water storage data: A review. *Surveys in Geophysics*, *44*(5), 1489–1517. https://doi.org/10.1007/s10712-022-09754-9

Jungclaus, J. H., Fischer, N., Haak, H., Lohmann, K., Marotzke, J., Matei, D., et al. (2013). Characteristics of the ocean simulations in the Max Planck Institute Ocean Model (MPIOM) the ocean component of the MPI–Earth system model. *Journal of Advances in Modeling Earth Systems*, *5*(2), 422–446. https://doi.org/10.1002/jame.20023

Kasevich, M., & Chu, S. (1991). Atomic interferometry using stimulated Raman transitions. *Physical Review Letters*, *67*(2), 181–184. https://doi.org/10.1103/PhysRevLett.67.181

Knabe, A., Schilling, M., Wu, H., HosseiniArani, A., Müller, J., Beaufils, Q., & Pereira dos Santos, F. (2022). The benefit of accelerometers based on cold atom interferometry for future satellite gravity missions. In J. Freymueller & L. Sanchez (Eds.), *Geodesy for a Sustainable Earth* (Vol. 154, pp. 213–220). Springer. https://doi.org/10.1007/1345_2022_151

Kupriyanov, A., Reis, A., Knabe, A., Fletling, N., HosseiniArani, A., Romeshkani, M., et al. (2024). *Analysis of novel sensors and satellite formation flights for future gravimetry missions*. International Association of Geodesy Symposia. https://doi.org/10.1007/1345_2024_279

Kupriyanov, A., Reis, A., Schilling, M., Müller, V., & Müller, J. (2024). Benefit of enhanced electrostatic and optical accelerometry for future gravimetry missions. *Advances in Space Research*, *73*(6), 3345–3362. https://doi.org/10.1016/j.asr.2023.12.067

Lan, S.-Y., Kuan, P.-C., Estey, B., Haslinger, P., & Müller, H. (2012). Influence of the coriolis force in atom interferometry. *Physical Review Letters*, *108*(9), 090402. https://doi.org/10.1103/PhysRevLett.108.090402

Lecomte, H., Rosat, S., Mandea, M., & Dumberry, M. (2023). Gravitational constraints on the Earth's inner core differential rotation. *Geophysical Research Letters*, *50*(23), e2023GL104790. https://doi.org/10.1029/2023GL104790

Lévèque, T., Fallet, C., Lefebve, J., Piquereau, A., Gauguet, A., Battelier, B., et al. (2022). CARIOQA: Definition of a quantum pathfinder mission. In K. Minoglou, N. Karafolas, & B. Cugny (Eds.), *International conference on space optics — icso 2022*. SPIE. https://doi.org/10.1117/12.2690536

Lévèque, T., Fallet, C., Mandea, M., Biancale, R., Lemoine, J. M., Tardivel, S., et al. (2021). Gravity field mapping using laser coupled quantum accelerometers in space. *Journal of Geodesy*, *95*(1), 15. https://doi.org/10.1007/s00190-020-01462-9

Lévèque, T., Gauguet, A., Michaud, F., Dos Santos, F. P., & Landragin, A. (2009). Enhancing the area of a Raman atom interferometer using a versatile double-diffraction technique. *Physical Review Letters*, *103*(8), 080405. https://doi.org/10.1103/physrevlett.103.080405

Liu, Y., Li, J., Xu, X., Wei, H., Li, Z., & Zhao, Y. (2024). Simulation analysis of recovering time-varying gravity fields based on Starlink-like constellation. *Geophysical Journal International*, *239*(1), 402–418. https://doi.org/10.1093/gji/ggae273

Loomis, B. D., Rachlin, K. E., & Luthcke, S. B. (2019). Improved Earth oblateness rate reveals increased ice sheet losses and mass-driven sea level rise. *Geophysical Research Letters*, *46*(12), 6910–6917. https://doi.org/10.1029/2019GL082929

Loomis, B. D., Rachlin, K. E., Wiese, D. N., Landerer, F. W., & Luthcke, S. B. (2020). Replacing GRACE/GRACE-FO with satellite laser ranging: Impacts on antarctic ice sheet mass change. *Geophysical Research Letters*, *47*(3), e2019GL085488. https://doi.org/10.1029/2019GL085488

Lyard, F. H., Allain, D. J., Cancet, M., Carrère, L., & Picot, N. (2021). FES2014 global ocean tide atlas: Design and performance. *Ocean Science*, *17*(3), 615–649. https://doi.org/10.5194/os-17-615-2021

Mandea, M., Dehant, V., & Cazenave, A. (2020). GRACE–gravity data for understanding the deep Earth's interior. *Remote Sensing*, *12*(24), 4186. https://doi.org/10.3390/rs12244186

Marque, J.-P., Christophe, B., & Foulon, B. (2010). Accelerometers of the GOCE mission: Return of experience from one year of in-orbit. In *Esa living planet symposium* (Vol. 686).57

Migliaccio, F., Pereira Dos Santos, F., Aguilera, D., Battelier, B., & Bouyer, P. (2022). Hybrid quantum-classical accelerometry for future space gravimetry missions. In *Proceedings of esa's living planet symposium 2022* (pp. 1–9).

Migliaccio, F., Reguzzoni, M., Batsukh, K., Tino, G. M., Rosi, G., Sorrentino, F., et al. (2019). Mocass: A satellite mission concept using cold atom interferometry for measuring the Earth gravity field. *Surveys in Geophysics*, *40*(5), 1029–1053. https://doi.org/10.1007/s10712-019-09566-4

Müntinga, H., Ahlers, H., Krutzik, M., Wenzlawski, A., Arnold, S., Becker, D., et al. (2013). Interferometry with bose-einstein condensates in microgravity. *Physical Review Letters*, *110*(9), 093602. https://doi.org/10.1103/PhysRevLett.110.093602

Pail, R., Bingham, R., Braitenberg, C., Dobslaw, H., Eicker, A., Güntner, A., et al., and IUGG Expert Panel. (2015). Science and user needs for observing global mass transport to understand global change and to benefit society. *Surveys in Geophysics*, *36*(6), 743–772. https://doi.org/10.1007/s10712-015-9348-9

Savcenko, R., & Bosch, W. (2012). EOT11a-empirical ocean tide model from multi-mission satellite altimetry. Report No. 89. *DGFI*. https://doi.org/10.1594/PANGAEA.834232

Scanlon, B. R., Fakhreddine, S., Rateb, A., de Graaf, I., Famiglietti, J., Gleeson, T., et al. (2023). Global water resources and the role of groundwater in a resilient water future. *Nature Reviews Earth and Environment*, *4*(2), 87–101. https://doi.org/10.1038/s43017-022-00378-6

Schilling, M., Wodey, E., Timmen, L., Tell, D., Zipfel, K. H., Schlippert, D., et al. (2020). Gravity field modelling for the Hannover 10 m atom interferometer. *Journal of Geodesy*, *94*(12), 122. https://doi.org/10.1007/s00190-020-01451-y

Shihora, L., Balidakis, K., Dill, R., Dahle, C., Ghobadi-Far, K., Bonin, J., & Dobslaw, H. (2022). Non–tidal background modeling for satellite gravimetry based on operational ECWMF and ERA5 reanalysis data: AOD1B RL07. *Journal of Geophysical Research: Solid Earth*, *127*(8), e2022JB024360. https://doi.org/10.1029/2022JB024360

Shihora, L., Liu, Z., Balidakis, K., Wilms, J., Dahle, C., Flechtner, F., et al. (2024). Accounting for residual errors in atmosphere–ocean background models applied in satellite gravimetry. *Journal of Geodesy*, *98*(4), 1–13. https://doi.org/10.1007/s00190-024-01832-7

Tapley, B. D., Watkins, M. M., Flechtner, F., Reigber, C., Bettadpur, S., Rodell, M., et al. (2019). Contributions of GRACE to understanding climate change. *Nature Climate Change*, *9*(5), 358–369. https://doi.org/10.1038/s41558-019-0456-2

Templier, S., Lefèvre, G., Battelier, B., & Bouyer, P. (2022). A quantum accelerometer triad for navigation and positioning. *Nature Communications*, *13*, 337.

Tennstedt, B. (2025). Concept and evaluation of a hybridization scheme for atom interferometers and inertial measurement units (Doctoral dissertation, Leibniz Universität Hannover). https://doi.org/10.15488/18303

Tennstedt, B., Rajagopalan, A., Weddig, N. B., Abend, S., Schön, S., & Rasel, E. M. (2023). *Atom strapdown: Toward integrated quantum inertial navigation* (Vol. 70). NAVIGATION: Journal of the Institute of Navigation. https://doi.org/10.33012/navi.604. 604

Weddig, N. B., Tennstedt, B., & Schön, S. (2021). Performance evaluation of a three-dimensional cold atom interferometer based inertial navigation system. In P. Hecker (Ed.), *2021 DGON Inertial Sensors and Systems (ISS)* (pp. 1–20). IEEE. https://doi.org/10.1109/ISS52949.2021.9619776

Wiese, D. N., Bienstock, B., Blackwood, C., Chrone, J., Loomis, B. D., Sauber, J., et al. (2022). The mass change designated observable study: Overview and results. *Earth and Space Science*, *9*(8), e2022EA002311. https://doi.org/10.1029/2022EA002311

Wöske, F., Kato, T., Rievers, B., & List, M. (2019). GRACE accelerometer calibration by high precision non-gravitational force modeling. *Advances in Space Research*, *63*(3), 1318–1335. https://doi.org/10.1016/j.asr.2018.10.025

Wu, H. (2016). *Gravity field recovery from GOCE observations (Dissertation)*. Leibniz Universität Hannover.

Xie, Y., Fan, B., Li, H., Liang, A., Huang, M., Wu, B., et al. (2022). Ground experiment verification and on-orbit prediction of the two-stage cooling at pK level in the Chinese space station. *Journal of Physics B: Atomic, Molecular and Optical Physics*, *55*(20), 205301. https://doi.org/10.1088/1361-6455/ac8e3d

Zahzam, N., Christophe, B., Bresson, A., Battelier, B., & Bouyer, P. (2022). Hybrid electrostatic-atomic accelerometer for future gravity missions. *Physical Review Applied*, *17*(2), L1959–L1964.

Zahzam, N., Christophe, B., Lebat, V., Hardy, E., Huynh, P.-A., Marquet, N., et al. (2022). Hybrid electrostatic-atomic accelerometer for future space gravity missions. *Remote Sensing*, *14*(14), 3273. https://doi.org/10.3390/rs14143273

Zingerle, P., Romeshkani, M., Haas, J., Gruber, T., Güntner, A., Müller, J., & Pail, R. (2024). The benefits of future quantum accelerometers for satellite gravimetry. *Earth and Space Science*, *11*(9), e2024EA003630. https://doi.org/10.1029/2024EA003630